Diagnostic significance of the checkpoint kinase 1 gene in high-grade gastroenteropancreatic neuroendocrine neoplasms

NA LI, JIANDUO AN and YANPING HU

Department of Pathology, Beijing Luhe Hospital, Capital Medical University, Beijing 101100, P.R. China

Received May 18, 2025; Accepted October 7, 2025

DOI: 10.3892/etm.2025.13001

Abstract. The diagnosis of high-grade gastroenteropancreatic neuroendocrine neoplasms (HG-GEP NENs) primarily relies on histopathological differentiation and mitotic count assessment. Due to interobserver variability in morphological evaluation, reliable molecular diagnostic biomarkers are needed to support accurate classification, particularly in challenging cases where the distinction between well-differentiated neuroendocrine tumours grade 3 (NET G3) and poorly differentiated neuroendocrine carcinoma (NEC) is ambiguous. The present study aimed to identify clinicopathological markers that facilitate the differential diagnosis of HG-GEP NENs. A total of 34 patients with HG-GEP NENs were included in study. Integrated bioinformatics analysis, including protein-protein interaction network construction from the GSE211485 dataset and subsequent validation using The Cancer Genome Atlas data, identified checkpoint kinase 1 (*CHEK1*) as a potential molecular marker for diagnosing HG-GEP NENs, which also showed prognostic significance in digestive system tumours. Despite no significant difference in overall *CHEK1* DNA levels between groups, high *CHEK1* expression was significantly more prevalent in the NEC group than in the NET G3 group (P=0.0113), with the small cell NEC (SCNEC) subgroup exhibiting the highest frequency (P=0.0075). Receiver operating characteristic curve analysis results revealed that high *CHEK1* expression distinguished NEC from NET G3 [area under the curve (AUC)=0.8029]. When further stratified, its diagnostic performance was more pronounced for SCNEC (AUC=0.8708) than for large cell NEC (AUC=0.7102). These findings suggest that *CHEK1* may serve as a potential molecular biomarker for the differential diagnosis of HG-GEP NENs. Although further large-scale clinicopathological studies are needed, *CHEK1* expression demonstrates diagnostic potential and could be utilised to inform standard treatment plans.

Correspondence to: Professor Yanping Hu, Department of Pathology, Beijing Luhe Hospital, Capital Medical University, 82 South Xinhua Road, Tongzhou, Beijing 101100, P.R. China
E-mail: yphu@163.com

Abbreviations: AUC, area under the curve; *CHEK1*, checkpoint kinase 1; DEGs, differentially expressed genes; FFPE, formalin-fixed paraffin-embedded; GEP-NEN, gastroenteropancreatic neuroendocrine neoplasm; GO, Gene Ontology; HG-GEP NEN, high-grade GEP NEN; KEGG, Kyoto Encyclopaedia of Genes and Genomes; NEC, neuroendocrine carcinoma; LCNEC, large cell NEC; LG-GEP NEN, low-grade GEP NEN; NET, neuroendocrine tumour; NET G1, NET grade 1; NET G2, NET grade 2; NET G3, NET grade 3; PPI, protein-protein interaction; ROC, receiver operating characteristic; SCNEC, small cell NEC; TCGA, The Cancer Genome Atlas; WHO, World Health Organization

Key words: HG-GEP NEN, NET G3, *CHEK1*, diagnostic analysis, prognostic analysis

Introduction

Gastroenteropancreatic neuroendocrine neoplasms (GEP-NENs) are a heterogeneous group of tumours that originate from neuroendocrine cells within the gastrointestinal tract and pancreas, which possess hormone-secreting functions (1). Within the gastrointestinal tract, these cells are responsible for the secretion of digestive hormones such as gastrin, glucagon and secretin. In the pancreas, the endocrine cell population includes islet cells (such as α-cells and β-cells), which produce hormones, such as insulin and glucagon (2). In the 5th Edition of the World Health Organization (WHO) classification of digestive system tumours published in 2019 (3), GEP-NENs were classified as well-differentiated neuroendocrine tumours (NET) grade 1 (NET G1), NET grade 2 (NET G2) and poorly differentiated neuroendocrine carcinoma (NEC), with a high-grade designation defined by a Ki-67 proliferation index of >20% and a mitotic count of >20 per 2 mm^2. This classification system further stratified GEP-NENs into low-grade (LG) NENs, including NET G1 and NET G2, and high-grade (HG) NENs, including NET grade 3 (NET G3) and NEC. In the HG group, NET G3 (previously referred to as 'high-proliferative NET') are classified as well-differentiated neoplasms exhibiting morphological features similar to LG NET, but with a Ki-67 proliferation index of >20% (typically <55%). By contrast, NEC is characterised as a poorly differentiated, high-grade malignancy composed of either small or large cells, including small cell NEC (SCNEC) and large-cell NEC (LCNEC).

Further subclassification of NET G3 or NEC with a Ki-67 proliferation index of >20% may be necessary (4-6). Notable differences in biological behaviour, treatment approaches and

prognosis have been observed between NET G3 subgroups with Ki-67 index values of 20-55% and those with >55%. For instance, the subgroup with a Ki-67 >55% is associated with significantly shorter median overall survival time and typically requires platinum-based chemotherapy, unlike the subgroup with a Ki-67 of 20-55%, which is managed with systemic non-platinum regimens (5-8). Despite the existence of well-defined criteria, HG-NENs exhibit substantial heterogeneity owing to the distinct pathological and molecular characteristics. These molecular differences, which are explored in the following section, fundamentally underpin the pathological distinction between well-differentiated NET G3 and poorly differentiated NEC (9-11). These histological subtypes vary considerably in epidemiology, treatment strategies and clinical outcomes, reflecting their diverse biological behaviours (3). Advances in tumour immunology and molecular pathology have led to the development of novel therapeutic approaches for HG-GEP NENs, including molecular targeted therapies and immune checkpoint inhibitors, such as programmed cell death protein 1 inhibitors (12). However, the selection and evaluation of appropriate treatment options require a comprehensive assessment of multiple factors, such as tumour grade and stage, cellular differentiation, primary tumour site, Ki-67 proliferation index, molecular and immunohistochemical markers and NEC subtype.

Advancements in molecular pathology have indicated that HG-NENs have distinct molecular pathogenic mechanisms. Whole-genome studies have identified at least four functional pathways implicated in the molecular alterations of pancreatic NET: DNA damage repair (involving genes such as *MUTYH, CHEK2* and *BRCA2*), chromatin remodelling (including *ARID1A* and *SMARCA4*), telomere maintenance (notably *DAXX* and *ATRX* genes) and the PI3K/mechanistic target of rapamycin signalling pathway (involving *EWSR* fusion, *PTEN* and *HIF1/2*) (10,11,13,14). In rectal NET, recurrent mutations have been reported in genes such as *TP53*, *PTEN*, *CDKN2A*, *FBXW7* and *AKT1*, with the mutational burden shown to increase with tumour grade. However, the specific roles of the Ras/Raf/MAPK and PI3K/AKT pathways in the pathogenesis of rectal NET remain unclear (14-16). Conversely, NEC exhibit entirely different molecular profiles from GEP-NET. The most frequently altered genes in GEP-NEC include *TP53*, *RB1*, *KRAS*, *BRAF* and *APC*. In GEP-NET, *RB1* mutations are absent (14,17,18). While recurrent *TP53* mutations have been identified in certain subtypes, such as rectal NET, they remain uncommon across the broader spectrum of GEP-NET; when present outside the rectum, they are typically confined to a subset of NET G3 (16).

CHEK1 is a crucial protein-coding gene in the human genome (19). *CHEK1* functions as a key regulatory factor involved in cell cycle control, DNA damage repair and apoptosis inhibition (19-21); this is essential for proper cell division and the maintenance of genomic stability. The *CHEK1*-encoded protein belongs to the protein kinase family and primarily monitors and facilitates DNA damage repair within cells. *CHEK1* has been implicated in various malignancies (20-22), including colorectal cancer (23), multiple myeloma (24), hepatocellular carcinoma (25), lung adenocarcinoma (26) and lung squamous cell carcinoma (27). *CHEK1* exhibits a dual role in tumour progression: While it functions as a tumour suppressor in normal physiology by safeguarding genomic integrity, it is paradoxically co-opted in the neoplastic state to promote cell survival and induce therapy resistance. Aberrant activation or overexpression of *CHEK1* can suppress apoptosis and promote DNA repair, thereby enhancing tumour cell survival and increasing resistance to therapeutic interventions (19,20).

Over the years, *CHEK1* has received considerable attention in the field of tumour biology and the development of therapeutic strategies, emerging as a potential therapeutic target (21,22,28,29). Several *CHEK1*-targeted inhibitors have been developed, including SRA737 (28), MK-8776 (VX-970) (29), LY2603618 (21), AZD7762 (30) and LY2606368 (27). These inhibitors disrupt the tumour cell cycle, thereby suppressing tumour cell proliferation, and have been experimentally validated in various malignancies. Specifically, LY2606368, AZD7762 and SRA737 have demonstrated efficacy in preclinical models of gastrointestinal tumours, including colorectal cancer, pancreatic cancer, GEP-NENs and small cell lung cancer. Additionally, MK-8776 (VX-970), LY2603618 and AZD7762 have demonstrated therapeutic potential in *in vitro* and *in vivo* models of digestive system tumours (21,27-30). The ability of *CHEK1* inhibitors to effectively suppress tumour cell growth and migration underscores their potential as viable therapeutic agents.

Despite its well-established role in various malignancies, the involvement of *CHEK1* in HG-GEP NENs remains largely uncharacterised. Previous studies have highlighted the dual role of *CHEK1* in tumourigenesis. The same mechanism, *CHEK1*-mediated cell-cycle arrest, serves opposite purposes. In normal cells it functions as a tumour-suppressive process that preserves genomic integrity by permitting DNA repair, whereas in cancer cells it is co-opted as a pro-survival mechanism that enables tumour cells to withstand replication stress or therapeutic pressure (19,21). Given the dual role of *CHEK1* as a key regulatory protein downstream of MEK/ERK signalling (31) and as a central effector of the DNA-damage response (19), the *CHEK1* overexpression observed in NEC, an attribute correlated with aggressive behaviour, supports its potential utility as a molecular biomarker for subtyping HG-GEP NENs (12).

The present study aimed to elucidate the clinical and biological significance of *CHEK1* in HG-GEP NENs, using a combination of public transcriptomic data [Gene Expression Omnibus (GEO): GSE211485] and an institutional cohort of 38 patient-derived formalin-fixed paraffin-embedded (FFPE) tissue samples. Differentially expressed genes (DEGs) were initially identified through transcriptomic analysis, followed by validation of *CHEK1* expression in tumour tissue samples. An overview of the study workflow is illustrated in Fig. 1A. Furthermore, the potential role of *CHEK1* in the pathogenesis and progression of HG-GEP NENs was explored through associations with histological subtypes and clinicopathological parameters. The specific objectives of the present study were to: i) Determine the differential expression of *CHEK1* among histologically distinct HG-GEP NENs subtypes; ii) explore its potential contribution to tumour biology; iii) assess its diagnostic and prognostic utility; and iv) provide a rationale for the future development of *CHEK1*-targeted therapeutic strategies in this rare but aggressive disease.

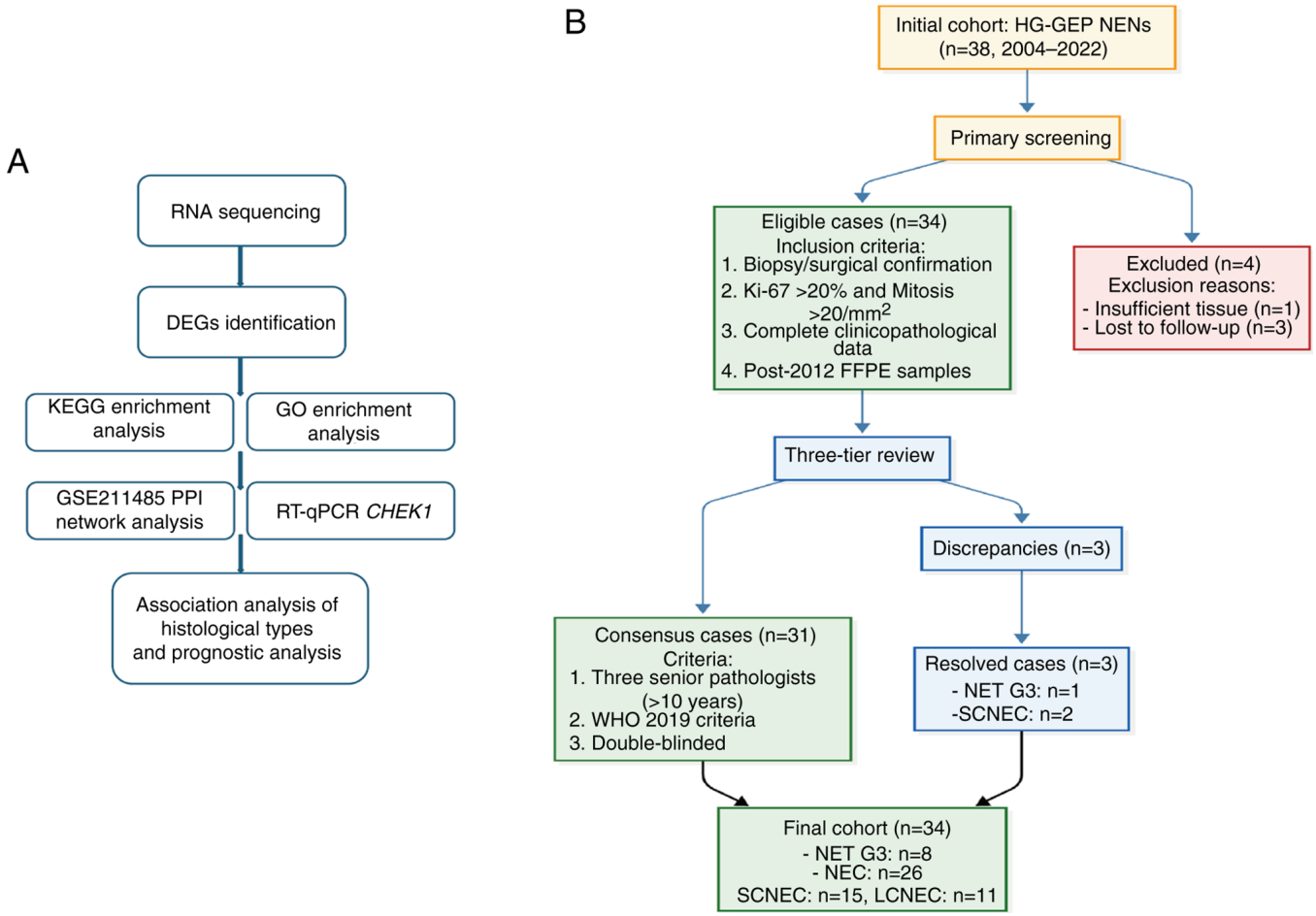

Figure 1. Workflow diagram and case selection flowchart. (A) Workflow of the study. (B) Case inclusion and screening flowchart. DEGs, differentially expressed genes; KEGG, Kyoto Encyclopaedia of Genes and Genomes; GO, Gene Ontology; PPI, protein-protein interaction; RT-qPCR, reverse transcription-quantitative PCR; HG-GEP NENs, high-grade gastroenteropancreatic neuroendocrine neoplasms; FFPE, formalin-fixed paraffin-embedded; NET G3, neuroendocrine tumour grade 3; NEC, neuroendocrine carcinoma; SCNEC, small cell NEC; LCNEC, large-cell NEC; WHO, World Health Organisation; *CHEK1*, checkpoint kinase 1.

Materials and methods

Patient selection. The present study consecutively enrolled 38 patients with HG-GEP NENs who underwent diagnostic or therapeutic procedures (biopsy, puncture, surgery and/or consultation) at Beijing Luhe Hospital, Capital Medical University (Beijing, China) between January 2004 and May 2022. Inclusion criteria were as follows: i) Histopathologically confirmed HG-GEP NENs according to the WHO Classification Of Tumours Of The Digestive System (5th Edition, 2019) (3); ii) availability of complete clinical data with a follow-up duration of >1 year; and iii) availability of FFPE tumour tissue samples obtained after 2012 for molecular analysis. Patients not meeting all these criteria were excluded. The FFPE tissues obtained during routine clinical practice throughout this period were utilized for analysis. The cohort consisted of 9 patients with NET G3 (7 male patients and 2 female patients; median age, 66.0±12.4 years). In addition, the cohort also consisted of 29 patients with NEC who were further stratified into: i) LCNEC, 11 cases (5 male patients and 6 female patients; median age, 65.0±12.1 years); and ii) SCNEC, 18 cases (10 male patients and 8 female patients; median age, 65.0±9.6 years). The overall population included 22 male patients and 16 female patients (age range, 43-86 years; median age, 65.0±10.6 years). All patients were independently reviewed and classified by three senior pathologists according to the diagnostic criteria of the WHO classification of tumours of the digestive system (5th edition, 2019) (3). Any diagnostic discrepancies were resolved through multitiered consensus discussions (Fig. 1B). Pathological grading was performed based on comprehensive histopathological evaluation. Clinical follow-up data regarding recurrence, metastasis and survival status were obtained through telephone interviews, with the follow-up period extending from the date of initial tumour diagnosis until patient death. Complete follow-up data were available for 35 patients, while 3 cases were lost to follow-up. A total of 23 deaths were documented. Ethics approval was provided by the Institutional Review Board of Beijing Luhe Hospital, Capital Medical University (approval no. 2024-LHKY-107-01).

Identification of DEGs. Soldevilla *et al* (32) conducted transcriptome analyses via next-generation sequencing on a cohort comprising 84 tumour tissue samples from NENs of pulmonary and GEP origin. The resulting gene dataset (GSE211485) was made publicly available through the GEO database

(https://www.ncbi.nlm.nih.gov/geo/). In that study, 15 patients diagnosed with GEP NET-G1 and GEP NET-G2 were assigned to the LG-GEP NENs group, whereas 2 patients diagnosed with GEP-NEC were assigned to the HG-GEP NENs group. The present study analysed this dataset and DEG expression was assessed using R Studio (version 2023.12.1+402; Posit Software, PBC, Boston, MA, USA) and DESeq2 (version 1.40.2; Bioconductor Project). In this DESeq2 model where the HG-GEP NENs group served as the baseline, a negative log2FC indicates lower expression in the LG-GEP NENs group relative to the HG-GEP NENs group, signifying upregulation in the high-grade tumours. Batch effects were corrected using variance stabilising transformation. DEGs were identified based on dual screening criteria to ensure result reliability: i) Absolute log2 fold change (FC) >1 with a false discovery rate of <0.05; and ii) FC>2 or <0.5 with P<0.05.

Gene Ontology (GO) and Kyoto Encyclopaedia of Genes and Genomes (KEGG) enrichment analysis. GO and KEGG enrichment analyses of the identified DEGs were performed using the R package ClusterProfiler. GO enrichment analysis (http://geneontology.org/) was conducted across three domains: Biological processes, cellular components and molecular functions. KEGG enrichment analysis (https://www.genome.jp/kegg/) was performed to evaluate five domains: Metabolic pathways, signalling pathways, disease-related pathways, drug metabolism pathways and cellular processes.

Protein-protein interaction (PPI) network analysis. The identified DEGs were subjected to PPI network analysis. Network visualisation was conducted using the Search Tool for the Retrieval of Interacting Genes/Proteins database (version 12.0; https://string-db.org). Hub genes were identified using the CytoHubba plugin in Cytoscape (v3.10.1; https://cytoscape.org).

Prognostic analysis. A comprehensive analysis was conducted using data from The Cancer Genome Atlas (TCGA) database (https://portal.gdc.cancer.gov/), utilizing the TCGA-COAD and TCGA-READ datasets. Kaplan-Meier survival analysis was performed using the R package survival (version 3.5-7; https://cran.r-project.org/package=survival), with patients stratified into high- and low-expression groups based on the median expression level. The diagnostic performance of these genes was examined using receiver operating characteristic (ROC) curve analysis with the R package pROC (version 1.18.4; https://cran.r-project.org/package=pROC). Based on these prognostic and diagnostic analyses, *CHEK1* was identified as the key target gene with significant diagnostic and prognostic value.

Figures derived from TCGA-COAD and TCGA-READ were generated using the GEPIA2 online analysis platform (http://gepia2.cancer-pku.cn/).

RNA extraction and reverse transcription-quantitative PCR (RT-qPCR) detection. FFPE samples of patients diagnosed with HG-GEP NENs after 2012 were selected for *CHEK1* molecular detection. Four samples from patients diagnosed prior to 2012 (three SCNEC and one NET G3) were excluded from subsequent molecular analyses due to insufficient RNA quality or quantity, resulting in 34 cases being included in the RT-qPCR experiments. RNA was extracted from FFPE tissue samples using the Nucleic Acid Extraction Reagent (Model: FFPE RNA; cat. no. 8.02.0019; Xiamen Moyd Biotechnology Co., Ltd.,) according to the manufacturer's protocol. Sections 5-10 μm in thickness were placed in 1.5 ml DNase-/RNase-free centrifuge tubes. To remove paraffin, 1 ml xylene was added to each tube, followed by vortex mixing for 10 sec and incubation at 56˚C for 3 min. After a second vortex mix, the samples were centrifuged at 13,000 x g for 2 min at 24˚C, and the supernatant was discarded. This step was repeated if necessary to ensure complete deparaffinization. Dehydration was then performed by adding 1 ml absolute ethanol, vortexing and centrifuging at 13,000 x g for 2 min at 24˚C, after which the supernatant was discarded. The pellets were air-dried at 56˚C until no ethanol residue remained. For RNA purification, tissue lysis and digestion were initiated by adding 160 μl Buffer RTL and 20 μl Proteinase K Solution to the pellets. The samples were vortexed, briefly centrifuged at 13,000 x g for 10-15 sec at 24˚C and incubated at 56˚C for 30 min with agitation at 500 rpm, followed by a second incubation at 80˚C for 30 min with agitation at 500 rpm. After cooling to room temperature (~24˚C), on-site prepared DNase I working mixture (30 μl per sample) was added to digest genomic DNA, and the samples were incubated at 37˚C for 15 min. After centrifugation at 13,000 x g for 3 min at 24˚C, the entire supernatant was transferred to a new tube. A total of 340 μl Buffer RPB and 750 μl absolute ethanol was added, and the mixture was vortexed. The solution was transferred to an RNA spin column and centrifuged at 13,000 x g for 30 sec at 24˚C. The flow-through was discarded. The remaining solution was loaded and centrifuged again under the same conditions. The column was then washed sequentially with 600 μl Wash Buffer A and 600 μl Wash Buffer B, with centrifugation at 13,000 x g for 30 sec at 24˚C after each wash. After a final centrifugation at 13,000 x g for 3 min at 24˚C to dry the membrane, the RNA was eluted with 80-100 μl Buffer RTE mixture by incubation at 56˚C for 2 min and centrifugation at 13,000 x g for 1 min at 24˚C. The purified RNA was dissolved in RNase-free water, and its concentration and purity (A260/A280) were determined using a SMA4000 spectrophotometer (Merinton Instrument, Ltd.). cDNA was synthesized from the purified RNA using the TransScript cDNA Synthesis Kit (TransGen Biotech Co., Ltd.) according to the manufacturer's instructions. The reaction was performed under the following thermocycling conditions: 25˚C for 10 min, 42˚C for 15 min and 85˚C for 5 sec, followed by hold at 4˚C. For qPCR, each reaction contained 2 μl cDNA template, 10 μl SYBR Green qPCR Master Mix (Thermo Fisher Scientific Inc.), 0.4 μM of each forward and reverse primer and RNase-free water up to a total volume of 20 μl. The thermocycling conditions were as follows: Initial denaturation at 95˚C for 3 min, followed by 40 cycles of 95˚C for 15 sec, 60˚C for 30 sec and 72˚C for 30 sec. Amplification specificity was verified through melting curve analysis. A no-template control was included in each run to monitor potential contamination of the reaction. Target gene expression was normalised to the reference gene (*GAPDH*) threshold value, and the relative gene expression level was calculated using the $2^{-\Delta\Delta Cq}$ method (33).

Table I. Clinical characteristics of the patients from the GSE211485 dataset.

Characteristic	LG-GEP NENs		HG-GEP NENs
Grade	GEP NET-G1	GEP NET-G2	GEP NEC
Patient number	7	8	2
Sex (male/female), n	5/2	2/6	2/0
Primary tumour site			
Small intestine	2	4	0
Colon and rectum	1	2	1
Stomach	3	0	0
Pancreas	0	2	1
Appendix	1	0	0
Survival status			
Alive	6	5	0
Deceased	1	3	2

GEP, gastroenteropancreatic; NEN, neuroendocrine neoplasm; LG, low grade; HG, high grade; NET, neuroendocrine tumour; G1, grade 1; G2, grade 2; NEC, neuroendocrine carcinoma.

The primer sequences used for amplification of the target gene *CHEK1* and the reference gene *GAPDH* were as follows: *CHEK1* forward, 5'-GTGTCAGAGTCTCCCAGTGGAT-3' and reverse, 5'-GTTCTGGCTGAGAACTGGAGTAC-3'; and *GAPDH* forward, 5'-GGTGGTCTCCTCTGACTTCAACA-3' and reverse, 5'-GTTGCTGTAGCCAAATTCGTTGT-3'.

Statistical analysis. Transcriptomic (TPM) and corresponding clinical data were obtained from TCGA-COAD and TCGA-READ datasets, which were used as representative cohorts of digestive system tumours. Samples annotated as 'solid tissue normal' were included as adjacent non-tumourous tissues. As the numbers of tumour and normal samples were not identical, the comparison of *CHEK1* expression between tumour and adjacent normal tissues was performed using an unpaired two-tailed Student's t-test. Statistical analyses were performed using SPSS (version 29.0; IBM Corp.) and R Studio (version 2023.12.1+402; Posit Software). Categorical variables are presented as number (n) and percentage (%), while continuous variables are expressed as the mean ± standard deviation (SD) or median with interquartile range (IQR), as appropriate. For categorical analysis, gene expression levels were dichotomized into 'high' and 'low' groups based on the median expression value of the entire cohort. Descriptive statistics, including χ^2 and Fisher's exact tests were employed for data summarization and clinicopathological associations. Comparisons of continuous variables between two groups were performed using an unpaired two-tailed Student's t-test. For *CHEK1* quantitative analysis in the present cohort, which did not meet the assumptions of parametric tests, non-parametric tests were applied. Specifically, the Mann-Whitney U test was used for two-group comparisons, and the Kruskal-Wallis test followed by Dunn's post hoc test was used for comparisons across multiple groups. Survival assessment was conducted using Kaplan-Meier analysis and log-rank tests, whereas diagnostic performance was evaluated by ROC curve analysis. A post hoc power analysis was performed based on the quantitative RT-qPCR data of *CHEK1* expression using the R pwr package (effect size d=1.5), which demonstrated 65% statistical power. $P<0.05$ was considered to indicate a statistically significant difference.

Results

Patients. A total of 38 patients with HG-GEP NENs were included in the present study, comprising 9 patients (23.7%) with NET G3 and 29 patients (76.3%) with NEC. The NEC group was further subdivided into 11 patients (37.9% of NEC) with LCNEC and 18 patients (62.1% of NEC) with SCNEC. Complete follow-up data were available for 35 patients (92.1%), whereas data for 2 patients (5.3%) with NEC and 1 patient (2.6%) with NET G3 were unavailable. The median survival time for the entire cohort was 10.0 months (IQR, 5.0-25.0 months). When stratified by histological subtype, the median survival time was 25.0 months (IQR, 15.5-42.0 months) for the NET G3 group and 10.0 months (IQR, 5.0-21.5 months) for the NEC group. Analysis of clinicopathological data was conducted as described in our previous study (34). Immunohistochemical markers CLU and TP53 significantly impacted survival outcomes, with CLU serving as an independent prognostic factor. The immunohistochemical profile provided diagnostic value for NET G3 subtyping, while conventional demographic factors showed no significant associations with survival.

Identification of DEGs. Specimens from 17 patients were analysed from the GSE211485 dataset, including 15 patients with LG-GEP NENs and 2 patients with HG-GEP NENs. The baseline clinical characteristics of the patients are presented in Table I. Using DESeq2 with the HG-GEP NENs group designated as the baseline, a total of 18,591 genes were assessed. Comparative analysis identified 6 of these genes that were significantly upregulated in the HG-GEP NENs group compared with those in the LG-GEP NENs group (Fig. 2A; Table II). The complete list of these upregulated DEGs is provided in Table II.

Table II. Significantly upregulated DEGs in HG-GEP NENs compared with LG-GEP NENs.

Gene ID	Adjusted P-value	P-value	Log2 fold change
CENPF	0.0000298	1.25×10^{-9}	-2.1162718
CHEK1	0.0015899	1.52×10^{-7}	-1.1901370
RGPD3	0.0015899	2.00×10^{-7}	-1.6814988
UBE2T	0.0057300	9.60×10^{-7}	-1.6553494
E2F7	0.0210587	4.41×10^{-6}	-1.0386288
ITGB3BP	0.0465996	1.10×10^{-5}	-1.3835926

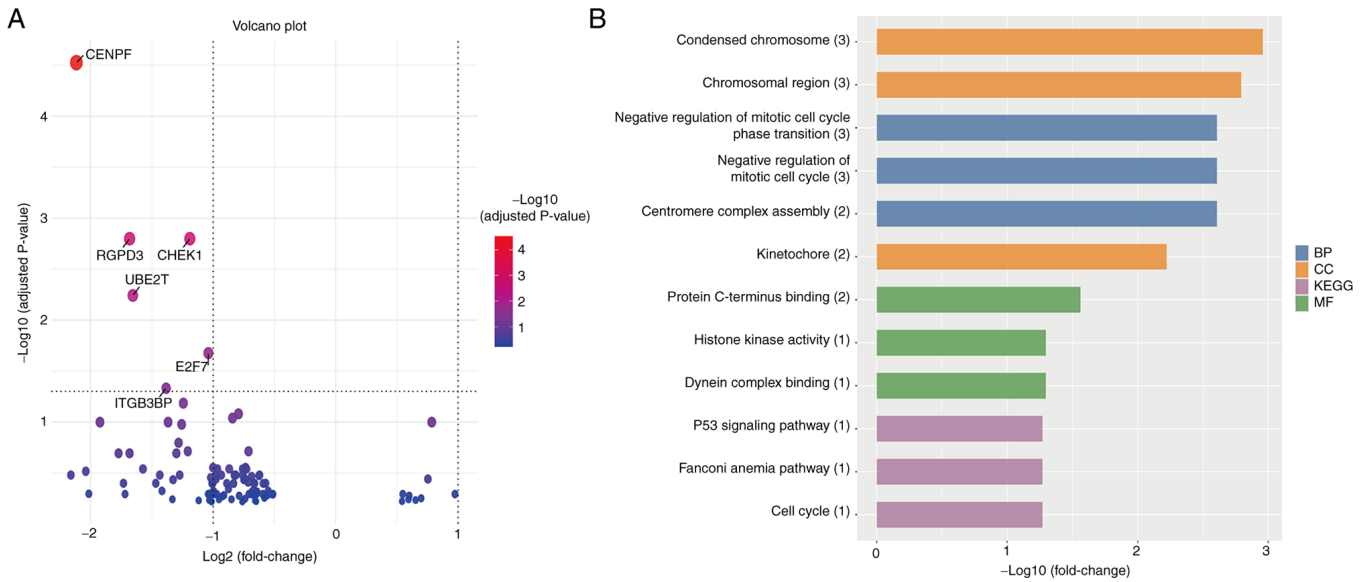

Figure 2. Overall analysis of the DEGs. (A) Volcano plot of the DEGs. Red and blue dots represent significantly upregulated and downregulated genes, respectively (adjusted P-value <0.05 and $|\log_2 FC|>1$). (B) GO and KEGG enrichment analysis of the DEGs. Bar plots show the top significantly enriched terms. The x-axis represents the enrichment significance [$-\text{Log}_{10}$(adjusted P-value)], and numbers in parentheses indicate gene counts for each term. DEGs, differentially expressed genes; BP, biological processes; CC, cellular component; MF, molecular function; KEGG, Kyoto Encyclopedia of Genes and Genomes.

GO and KEGG enrichment analysis of DEGs. GO enrichment analysis demonstrated significant enrichment of DEGs in biological processes related to 'centromere complex assembly', 'negative regulation of mitotic cell cycle' and 'negative regulation of mitotic cell cycle phase transition'; cellular components related to 'condensed chromosome', 'chromosomal region' and 'kinetochore'; and molecular functions related to 'protein C-terminus binding' , 'dynein complex binding', and 'histone kinase activity'. KEGG enrichment analysis revealed substantial enrichment in pathways associated with 'Cell cycle', 'p53 signalling pathway' and 'Fanconi anemia pathway' (Fig. 2B).

PPI network analysis of DEGs. Among the six significantly upregulated DEGs, five genes (*CENPF*, *CHEK1*, *UBE2T*, *E2F7* and *ITGB3BP)* formed a tightly interconnected hub module in the PPI network constructed using the STRING database (Fig. 3A and B). The identification of these hub genes reveals their functional involvement in cell cycle regulation and DNA damage repair pathways. Furthermore, the convergence of their upregulated expression and central network position highlights their coordinated role in promoting genomic instability and uncontrolled proliferation, which are key mechanisms underlying HG-GEP NENs progression. Collectively, these findings support the value of further investigating these hub genes as potential therapeutic targets.

Analysis using TCGA database. Owing to the rarity of HG-GEP NENs, corresponding tumour classifications were unavailable in TCGA. Therefore, transcriptomic and clinical data from TCGA-COAD and TCGA-READ projects were utilized as relevant proxies for digestive system tumours. Survival analysis demonstrated that high expression of *CHEK1* was significantly associated with poorer overall survival (Log-rank P<0.05; Fig. 4A-E). Concurrently, ROC curve analysis indicated that *CHEK1* expression possessed high diagnostic accuracy for distinguishing tumour from normal tissues (AUC >0.85; Fig. 4F). *CHEK1* was selected for further analysis since it emerged as the most prognostically and diagnostically significant gene among the five hub genes in these validation analyses. Among these, *CHEK1* was significantly overexpressed in digestive system tumour tissues compared with that in adjacent normal tissues based on

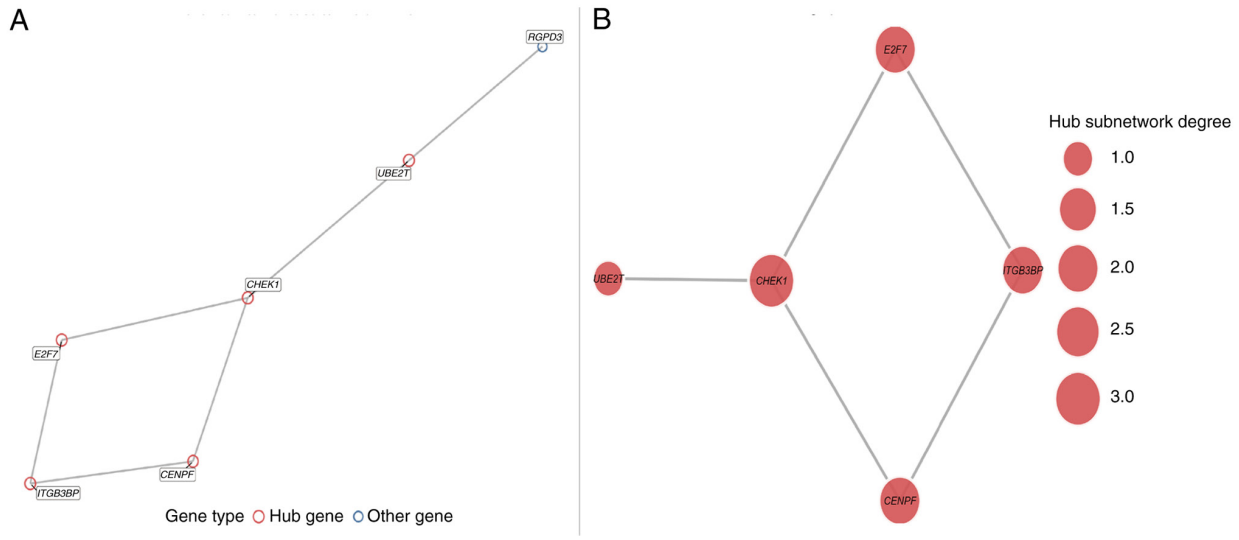

Figure 3. PPI network analysis of DEGs. (A) PPI network constructed from DEGs. (B) Five hub genes (*CHEK1*, *CENPF*, *UBE2T*, *E2F7* and *ITGB3BP*) were identified within the network. DEGs, differentially expressed genes; PPI, protein-protein interaction.

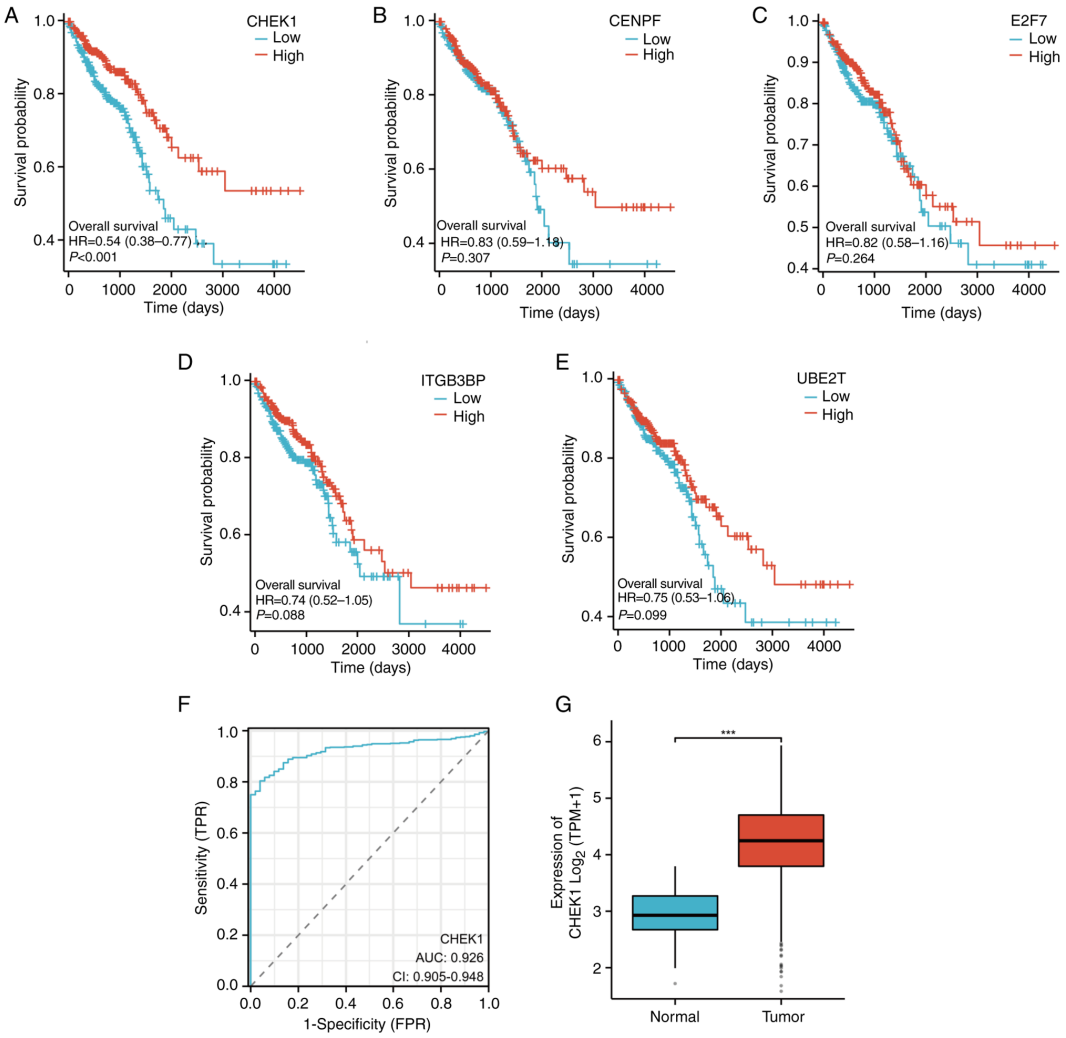

Figure 4. Prognostic and diagnostic analysis of the DEGs identified from the GSE211485 dataset. (A-E) Kaplan-Meier survival curves showing the association between the expression levels of the five identified DEGs (A) *CHEK1*, (B) *CENPF*, (C) *E2F7*, (D) *ITGB3BP* and (E) *UBE2T*, and overall survival in patients with digestive system tumours. The HR and 95% CIs were calculated using the log-rank test. (F) ROC curve showing the diagnostic performance of *CHEK1* expression for distinguishing tumour from normal tissues. The AUC indicates diagnostic accuracy. (G) Expression of *CHEK1* [log2 (TPM +1)] in digestive system tumour tissues compared with adjacent normal tissues. Statistical significance is indicated as ***P<0.001. DEGs, differentially expressed genes; CI, confidence interval; AUC, area under the curve; HR, hazard ratio; *CHEK1*, checkpoint kinase 1; FPR, false-positive rate; TPR, true-positive rate; TPM, transcripts per million.

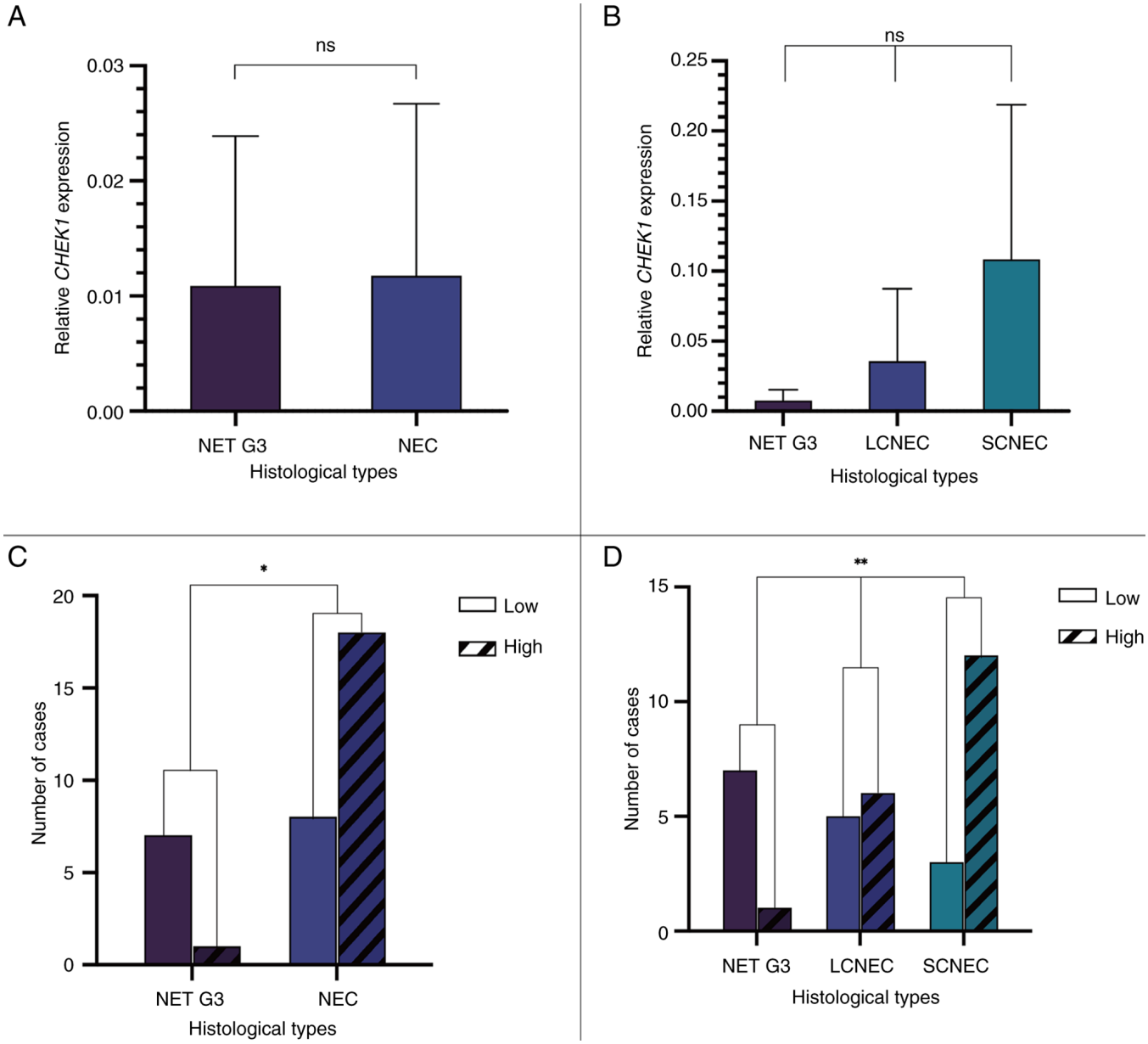

Figure 5. Reverse transcription-quantitative PCR results of *CHEK1* expression in high-grade gastroenteropancreatic neuroendocrine neoplasms. (A) Comparison of relative *CHEK1* mRNA expression levels between the NET G3 (n=8) and NEC (n=26) groups. (B) Comparison of relative *CHEK1* mRNA expression levels among the NET G3 (n=8), LCNEC (n=11) and SCNEC (n=15) subgroups. (C) Association between *CHEK1* expression status and histological types in NET G3 and NEC. (D) Association between *CHEK1* expression status and histological types in NET G3, LCNEC and SCNEC. *P<0.05 and **P<0.01. NET G3, neuroendocrine tumour grade 3; NEC, neuroendocrine carcinoma; LCNEC, large cell NEC; SCNEC, small cell NEC; *CHEK1*, checkpoint kinase 1; ns, not significant.

TCGA-COAD and TCGA-READ datasets (P<0.001, unpaired Student's t-test; Fig. 4G), suggesting that *CHEK1* may serve as a diagnostically and prognostically relevant target gene in digestive system malignancies.

RT-qPCR detection of CHEK1 expression in HG-GEP NENs. A total of 34 patients with HG-GEP NENs recruited in the present study were included in the RT-qPCR analysis, excluding 3 patients with SCNEC and 1 patient with NET G3 diagnosed prior to 2012. Patients were classified into high- and low-*CHEK1* expression groups based on the median expression level for categorical analyses. RT-qPCR analysis revealed that *CHEK1* expression was lower in the NET G3 group (n=8) compared with that in the NEC group (n=26), although the difference was not statistically significant (P=0.075; Fig. 5A). Further analysis among the NET G3 (n=8), LCNEC (n=11) and SCNEC (n=15) subgroups revealed no significant differences (P>0.05 for all pairwise comparisons; Fig. 5B). Analysis between histological subtypes indicated a significant difference between the NET G3 and NEC groups (P=0.0113; Fig. 5C), with a higher proportion of patients exhibiting high *CHEK1* expression in the NEC group. Further intergroup analysis demonstrated that the proportion of patients exhibiting elevated *CHEK1* expression was significantly higher in the SCNEC subgroup compared with that in the NET G3 and LCNEC groups (P=0.0075; Fig. 5D).

Table III. Diagnostic performance of *CHEK1* expression in high-grade gastroenteropancreatic neuroendocrine neoplasms.

Pathological category	AUC	Diagnostic efficacy
NEC (overall)	0.8029	Moderate diagnostic value
SCNEC	0.8708	Good diagnostic value
LCNEC	0.7102	Limited diagnostic value

NEC, neuroendocrine carcinoma; SCNEC, small cell NEC; LCNEC, large cell NEC; AUC, area under the curve.

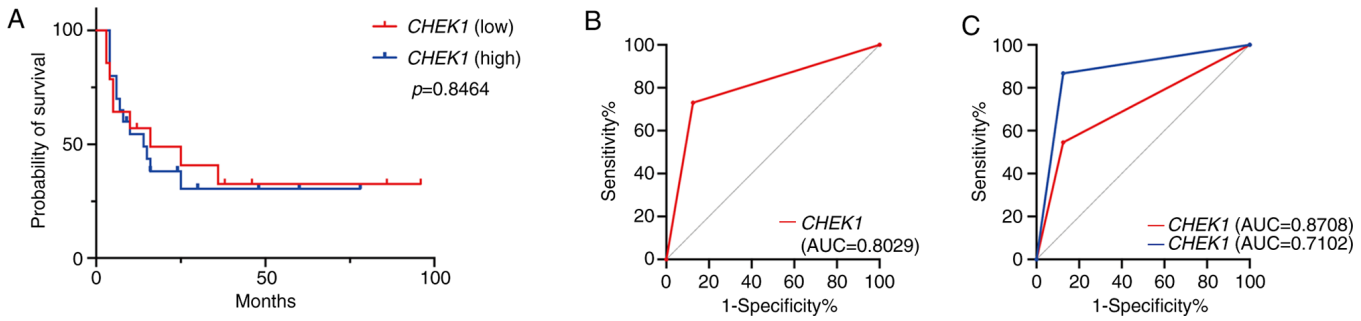

Figure 6. Prognostic and diagnostic value of *CHEK1* in HG-GEP NENs. (A) Kaplan-Meier analysis of overall survival in patients with HG-GEP NENs with high (n=14) vs. low (n=20) *CHEK1* expression (P=0.8464). (B) ROC curve analysis of *CHEK1* expression for distinguishing NEC from NET G3 (AUC=0.8029). (C) ROC curves of *CHEK1* expression for distinguishing LCNEC (AUC=0.7102) and SCNEC (AUC=0.8708) subtypes from the NET G3 group. HG-GEP NENs, high-grade gastroenteropancreatic neuroendocrine neoplasms; ROC, receiver operating characteristic; AUC, area under the curve; *CHEK1*, checkpoint kinase 1; NEC, neuroendocrine carcinoma; SCNEC, small cell NEC; LCNEC, large cell NEC.

Prognostic and diagnostic analysis of CHEK1 expression. The median survival time was 14 months in the *CHEK1* high-expression group and 16 months in the low-expression group. The Kaplan-Meier survival analysis demonstrated no significant difference in overall survival between the high- and low-expression groups (P=0.8464, Fig. 6A). ROC curve analysis demonstrated that high *CHEK1* expression influenced the diagnostic performance of NEC (AUC=0.8029; Fig. 6B). Further analysis, stratifying NEC cases into LCNEC and SCNEC subtypes, revealed that high *CHEK1* expression contributed to the diagnosis of LCNEC and SCNEC, with a more pronounced effect observed for SCNEC (AUC=0.8708) compared with LCNEC (AUC=0.7102) (Fig. 6C and Table III).

Discussion

The 2019 WHO Classification (5th Edition) introduced revised diagnostic criteria for HG-GEP NENs (3,5), defining them by a Ki-67 proliferation index of >20% and >20 mitoses per 2 mm^2. This revision underscores the dependence on histopathological morphology for precisely distinguishing NET G3 from NEC, a process susceptible to interobserver variability. The present study addresses this challenge by identifying a distinct molecular signature in HG-GEP NENs, characterized by the upregulation of cell cycle and DNA damage repair pathways. Critically, significant overexpression of *CHEK1* in NEC, particularly the SCNEC subtype, was demonstrated. This finding provides a molecular association for their aggressive clinical behaviours, aligning with established literature that associates NEC with poorer survival and platinum-based chemotherapy regimens, in contrast to NET G3 (7,10,35,36). Thus, the present findings not only validate the existing pathological distinction but also provide a molecular pathological basis for the divergent clinical phenotypes and treatment responses, potentially informing future targeted therapeutic strategies.

Macroscopically, NET G3 typically presents as solid nodules with a protruding or polypoid appearance, moderate firmness and grey-white or grey-yellow cut surface with well-defined borders relative to the surrounding tissues. Conversely, NEC often exhibit irregular ulcers or cauliflower-like protrusions, frequently accompanied by haemorrhage or necrosis. NEC are fragile, prone to fragmentation and are poorly demarcated from the adjacent tissues. When located in the colorectal region, such tumours commonly exhibit circumferential growth, leading to luminal narrowing and obstruction. Microscopically, NET G3 resemble well-differentiated NENs, characterised by organoid architectures or growth patterns such as trabecular, ribbon-like or glandular arrangements. Alternatively, NEC are defined by diffuse, sheet-like proliferation with pronounced cellular atypia, poor differentiation and frequent necrosis (3). In the present study, tumour specimens were reclassified in accordance with the latest WHO classification standards following a review by at least three senior pathologists.

The differential expression of specific immunohistochemical and molecular markers, such as somatostatin receptor 2A (SSTR2A), p53, Rb (36,37) and clusterin, may aid in distinguishing HG-GEP NENs (38). However, the identification of novel molecular biomarkers remains essential for improving differential diagnostic accuracy. This is particularly important

given that, due to the rarity of these neoplasms, most available data have been obtained from patients with NEC, with NET G3 being even less common. Furthermore, sequencing data within existing databases remain limited.

In the present study, *CHEK1* was identified as a novel complementary diagnostic marker in accordance with the WHO 2019 criteria, demonstrating concordance with established immunohistochemical markers (such as SSTR2A and p53) and *KRAS*/*BRAF* mutational profiles (34). However, two critical limitations warrant consideration. First, the transcriptomic dataset included only two HG cases, thereby limiting the representativeness of the sample. Second, due to the unavailability of HG-GEP NENs data in TCGA, broader digestive system tumour datasets were utilised for validation, which may have affected the specificity of the findings.

Given the rarity of HG-GEP NENs and the limitations of existing databases, several research priorities are proposed: i) The establishment of multicentre collaborative networks to ensure the inclusion of ≥20 cases per subtype (NET G3/LCNEC/SCNEC); ii) the implementation of standardised diagnostic and research protocols; and iii) the execution of integrated multi-omics analyses on HG-GEP NEN samples. Furthermore, validation at the protein level (such as through immunohistochemical analysis of *CHEK1* in HG-GEP NEN tissues) and functional assays using HG-GEP NEN-derived cell lines will be essential to elucidate the mechanistic role of *CHEK1* in cell cycle dysregulation. These comprehensive approaches will facilitate definitive validation of the diagnostic utility of *CHEK1* and deepen the understanding of its biological function in these neoplasms, thereby contributing to the development of more precise molecular classification systems.

In conclusion, the present study demonstrated the diagnostic value of *CHEK1*, thereby providing valuable insights and guidance for future clinical pathology research and practice. The findings suggest that *CHEK1* may serve as a novel molecular biomarker for the differential diagnosis of HG-GEP NENs. However, the small sample size represents a significant limitation of the present study, potentially restricting the immediate applicability of the findings to clinical practice. To fully elucidate the underlying molecular pathogenic mechanisms of the identified genes, further biological investigations are required. Moreover, large-scale clinicopathological studies are necessary before these findings can be translated into clinical practice.

Acknowledgements

Not applicable.

Funding

The present study was supported by the Beijing Tongzhou District Science and Technology Committee Project Fund (grant no. KJ2024CX027).

Availability of data and materials

The data generated in the present study may be requested from the corresponding author.

Authors' contributions

NL contributed to the study conceptualization, data curation, formal data analysis, experimental investigation, methodology development, validation of the results and writing of the original draft. YH contributed to the study conceptualization, project administration, funding acquisition, and reviewing and editing of the manuscript. JA performed experimental investigations and validated the experimental results. NL and YH confirm the authenticity of all the raw data. All authors have read and approved the final manuscript.

Ethics approval and consent to participate

This study was conducted in accordance with the ethical standards of the Declaration of Helsinki and was approved by the Institutional Review Board of Beijing Luhe Hospital, Capital Medical University (approval no. 2024-LHKY-107-01). The requirement for written informed consent was waived by the same ethics committee due to the retrospective nature of the study.

Patient consent for publication

Not applicable.

Competing interests

The authors declare that they have no competing interests.

References

1. Pavel M, Öberg K, Falconi M, Krenning EP, Sundin A and Perren A; ESMO Guidelines Committee: Electronic address: clinicalguidelines@esmo.org: Gastroenteropancreatic neuroendocrine neoplasms: ESMO clinical practice guidelines for diagnosis, treatment and follow-up. Ann Oncol 31: 844-860, 2020.
2. Gribble FM and Reimann F: Function and mechanisms of enteroendocrine cells and gut hormones in metabolism. Nat Rev Endocrinol 15: 226-237, 2019.
3. Nagtegaal ID, Odze RD, Klimstra D, Paradis V, Rugge M, Schirmacher P, Washington KM, Carneiro F and Cree IA; WHO Classification of Tumours Editorial Board: The 2019 WHO classification of tumours of the digestive system. Histopathology 76: 182-188, 2020.
4. Busico A, Maisonneuve P, Prinzi N, Pusceddu S, Centonze G, Garzone G, Pellegrinelli A, Giacomelli L, Mangogna A, Paolino C, *et al*: Gastroenteropancreatic high-grade neuroendocrine neoplasms: Histology and molecular analysis, two sides of the same coin. Neuroendocrinology 110: 616-629, 2020.
5. Milione M, Maisonneuve P, Pellegrinelli A, Grillo F, Albarello L, Spaggiari P, Vanoli A, Tagliabue G, Pisa E, Messerini L, *et al*: Ki67 proliferative index of the neuroendocrine component drives MANEC prognosis. Endocr Relat Cancer 25: 583-593, 2018.
6. Tang LH, Untch BR, Reidy DL, O'Reilly E, Dhall D, Jih L, Basturk O, Allen PJ and Klimstra DS: Well-differentiated neuroendocrine tumors with a morphologically apparent high-grade component: A pathway distinct from poorly differentiated neuroendocrine carcinomas. Clin Cancer Res 22: 1011-1017, 2016.
7. Sorbye H, Kong G and Grozinsky-Glasberg S: PRRT in high-grade gastroenteropancreatic neuroendocrine neoplasms (WHO G3). Endocr Relat Cancer 27: R67-R77, 2020.
8. Pellat A and Coriat R: Well differentiated grade 3 neuroendocrine tumors of the digestive tract: A narrative review. J Clin Med 9: 1677, 2020.
9. Venizelos A, Elvebakken H, Perren A, Nikolaienko O, Deng W, Lothe IMB, Couvelard A, Hjortland GO, Sundlöv A, Svensson J, *et al*: The molecular characteristics of high-grade gastroenteropancreatic neuroendocrine neoplasms. Endocr Relat Cancer 29: 1-14, 2021.

10. Scarpa A, Chang DK, Nones K, Corbo V, Patch AM, Bailey P, Lawlor RT, Johns AL, Miller DK, Mafficini A, *et al*: Whole-genome landscape of pancreatic neuroendocrine tumours. Nature 543: 65-71, 2017.
11. Mafficini A and Scarpa A: Genetics and epigenetics of gastroenteropancreatic neuroendocrine neoplasms. Endocr Relat Cancer 26: R249-R266, 2019.
12. Jin XF, Spöttl G, Maurer J, Nölting S and Auernhammer CJ: Antitumoral activity of the MEK inhibitor trametinib (TMT212) alone and in combination with the CDK4/6 inhibitor ribociclib (LEE011) in neuroendocrine tumor cells in vitro. Cancers (Basel) 13: 1485, 2021.
13. Wang ZJ, An K, Li R, Shen W, Bao MD, Tao JH, Chen JN, Mei SW, Shen HY, Ma YB, *et al*: Analysis of 72 patients with colorectal high-grade neuroendocrine neoplasms from three chinese hospitals. World J Gastroenterol 25: 5197-5209, 2019.
14. Uccella S, La Rosa S, Metovic J, Marchiori D, Scoazec JY, Volante M, Mete O and Papotti M: Genomics of high-grade neuroendocrine neoplasms: Well-differentiated neuroendocrine tumor with high-grade features (G3 NET) and neuroendocrine carcinomas (NEC) of various anatomic sites. Endocr Pathol 32: 192-210, 2021.
15. Mitsuhashi K, Yamamoto I, Kurihara H, Kanno S, Ito M, Igarashi H, Ishigami K, Sukawa Y, Tachibana M, Takahashi H, *et al*: Analysis of the molecular features of rectal carcinoid tumors to identify new biomarkers that predict biological malignancy. Oncotarget 6: 22114-22125, 2015.
16. Park HY, Kwon MJ, Kang HS, Kim YJ, Kim NY, Kim MJ, Min KW, Choi KC, Nam ES, Cho SJ, *et al*: Targeted next-generation sequencing of well-differentiated rectal, gastric, and appendiceal neuroendocrine tumors to identify potential targets. Hum Pathol 87: 83-94, 2019.
17. Hijioka S, Hosoda W, Matsuo K, Ueno M, Furukawa M, Yoshitomi H, Kobayashi N, Ikeda M, Ito T, Nakamori S, *et al*: Rb loss and KRAS mutation are predictors of the response to platinum-based chemotherapy in pancreatic neuroendocrine neoplasm with grade 3: A japanese multicenter pancreatic NEN-G3 study. Clin Cancer Res 23: 4625-4632, 2017.
18. Sorbye H, Baudin E and Perren A: The problem of high-grade gastroenteropancreatic neuroendocrine neoplasms. Endocrinol Metab Clin North Am 47: 683-698, 2018.
19. Patil M, Pabla N and Dong Z: Checkpoint kinase 1 in DNA damage response and cell cycle regulation. Cell Mol Life Sci 70: 4009-4021, 2013.
20. Qiu Z, Oleinick NL and Zhang J: ATR/CHK1 inhibitors and cancer therapy. Radiother Oncol 126: 450-464, 2018.
21. Hubackova S, Davidova E, Boukalova S, Kovarova J, Bajzikova M, Coelho A, Terp MG, Ditzel HJ, Rohlena J and Neuzil J: Replication and ribosomal stress induced by targeting pyrimidine synthesis and cellular checkpoints suppress p53-deficient tumors. Cell Death Dis 11: 110, 2020.
22. Jaaks P, Coker EA, Vis DJ, Edwards O, Carpenter EF, Leto SM, Dwane L, Sassi F, Lightfoot H, Barthorpe S, *et al*: Effective drug combinations in breast colon and pancreatic cancer cells. Nature 603: 166-173, 2022.
23. Pang YY, Chen ZY, Zeng DT, Li DM, Li Q, Huang WY, Li B, Luo JY, Chi BT, Huang Q, *et al*: Checkpoint kinase 1 in colorectal cancer: Upregulation of expression and promotion of cell proliferation. World J Clin Oncol 16: 101725, 2025.
24. Gu C, Wang W, Tang X, Xu T, Zhang Y, Guo M, Wei R, Wang Y, Jurczyszyn A, Janz S, *et al*: CHEK1 and circCHEK1_246aa evoke chromosomal instability and induce bone lesion formation in multiple myeloma. Mol Cancer 20: 84, 2021.
25. Sun J, Zhu Z, Li W, Shen M, Cao C, Sun Q, Guo Z, Liu L and Wu D: UBE2T-regulated H2AX monoubiquitination induces hepatocellular carcinoma radioresistance by facilitating CHK1 activation. J Exp Clin Cancer Res 39: 222, 2020.
26. Zuo W, Zhang W, Xu F, Zhou J and Bai W: Long non-coding RNA LINC00485 acts as a microRNA-195 sponge to regulate the chemotherapy sensitivity of lung adenocarcinoma cells to cisplatin by regulating CHEK1. Cancer Cell Int 19: 240, 2019.
27. Sen T, Tong P, Stewart CA, Cristea S, Valliani A, Shames DS, Redwood AB, Fan YH, Li L, Glisson BS, *et al*: CHK1 inhibition in small-cell lung cancer produces single-agent activity in biomarker-defined disease subsets and combination activity with cisplatin or olaparib. Cancer Res 77: 3870-3884, 2017.
28. Booth L, Roberts J, Poklepovic A and Dent P: The CHK1 inhibitor SRA737 synergizes with PARP1 inhibitors to kill carcinoma cells. Cancer Biol Ther 19: 786-796, 2018.
29. Cui Q, Cai CY, Wang JQ, Zhang S, Gupta P, Ji N, Yang Y, Dong X, Yang DH and Chen ZS: Chk1 inhibitor MK-8776 restores the sensitivity of chemotherapeutics in P-glycoprotein overexpressing cancer cells. Int J Mol Sci 20: 4095, 2019.
30. Landau HJ, McNeely SC, Nair JS, Comenzo RL, Asai T, Friedman H, Jhanwar SC, Nimer SD and Schwartz GK: The checkpoint kinase inhibitor AZD7762 potentiates chemotherapy-induced apoptosis of p53-mutated multiple myeloma cells. Mol Cancer Ther 11: 1781-1788, 2012.
31. Dai Y, Rahmani M, Pei XY, Khanna P, Han SI, Mitchell C, Dent P and Grant S: Farnesyltransferase inhibitors interact synergistically with the Chk1 inhibitor UCN-01 to induce apoptosis in human leukemia cells through interruption of both Akt and MEK/ERK pathways and activation of SEK1/JNK. Blood 105: 1706-1716, 2005.
32. Soldevilla B, Lens-Pardo A, Espinosa-Olarte P, Carretero-Puche C, Molina-Pinelo S, Robles C, Benavent M, Gomez-Izquierdo L, Fierro-Fernández M, Morales-Burgo P, *et al*: MicroRNA signature and integrative omics analyses define prognostic clusters and key pathways driving prognosis in patients with neuroendocrine neoplasms. Mol Oncol 17: 582-597, 2023.
33. Livak KJ and Schmittgen TD: Analysis of relative gene expression data using real-time quantitative PCR and the 2(-Delta Delta C(T)) method. Methods 25: 402-408, 2001
34. Li N, Hu Y, Wu L and An J: Clinicopathological correlations in 38 cases of gastroenteropancreatic high-grade neuroendocrine neoplasms. Front Oncol 14: 1399079, 2024.
35. Rosery V, Reis H, Savvatakis K, Kowall B, Stuschke M, Paul A, Dechêne A, Yang J, Zhao B, Borgers A, *et al*: Antitumor immune response is associated with favorable survival in GEP-NEN G3. Endocr Relat Cancer 28: 683-693, 2021.
36. Konukiewitz B, Schlitter AM, Jesinghaus M, Pfister D, Steiger K, Segler A, Agaimy A, Sipos B, Zamboni G, Weichert W, *et al*: Somatostatin receptor expression related to TP53 and RB1 alterations in pancreatic and extrapancreatic neuroendocrine neoplasms with a Ki67-index above 20. Mod Pathol 30: 587-598, 2017.
37. Bellizzi AM: Immunohistochemistry in the diagnosis and classification of neuroendocrine neoplasms: What can brown do for you? Hum Pathol 96: 8-33, 2020.
38. Czeczok TW, Stashek KM, Maxwell JE, O'Dorisio TM, Howe JR, Hornick JL and Bellizzi AM: Clusterin in neuroendocrine epithelial neoplasms: Absence of expression in a well-differentiated tumor suggests a jejunoileal origin. Appl Immunohistochem Mol Morphol 26: 94-100, 2018.